Hindawi
International Journal of Antennas and Propagation
Volume 2018, Article ID 9434360, 6 pages
https://doi.org/10.1155/2018/9434360

Research Article

A Compressive Sensing-Based Bistatic MIMO Radar Imaging Method in the Presence of Array Errors

Zhigang Liu, Jun Li, Junqing Chang, and Yifan Guo

National Lab of Radar Signal Processing, Xidian University, Xi'an 710071, China

Correspondence should be addressed to Jun Li; junli01@mail.xidian.edu.cn

Received 27 June 2018; Accepted 28 August 2018; Published 25 November 2018

Academic Editor: Andrea Francesco Morabito

A robust transmit-receive angle imaging method for bistatic MIMO radar based on compressed sensing is proposed. A new imaging model with array gain and phase error is established. The array gain error and phase error were modeled as a random interference for observation matrix by mathematical derivation. A constraint of observation matrix error is constructed in optimization problem of sparse recovery to reduce the effect of the interference of observation matrix. Then, the iterative algorithm of the optimization problems is derived. The proposed recovery method is more robust than the existed method in small samples, especially in the case of one snapshot. It is applicable in the case of relatively small array gain and phase errors. Simulation results confirm the effectiveness of the proposed method.

1. Introduction

Bistatic MIMO radar has the potential advantages of both bistatic radar and MIMO radar. Particularly, bistatic MIMO radar has the capability of obtaining the transmit angle information by processing the received data. As a new radar system, bistatic MIMO radar has been applied to target localization [1–4], clutter cancellation [5, 6], and imaging [7, 8]. Compressed sensing (CS) is attracted technique used in the field of radar imaging. Compressive sensing theory can achieve high-resolution imaging in small samples. Introduction of compressive sensing to bistatic MIMO radar can achieve more accurate imaging results. However, when the gain and phase errors exist in the array elements, the detection accuracy and imaging quality of the radar will deteriorate seriously. Many literatures have studied robust compression sensing recovery methods [7, 9–12]. A sparse recovery-based transmit-receive angle imaging scheme is proposed for bistatic multiple-input multiple-output (MIMO) radar in [8]. The method is robust under large error conditions. However, the method does not take into account the array phase error. Furthermore, it is not robust in the case of one snapshot. Therefore, it is necessary to further study the robust recovery method of bistatic MIMO radar in the nonideal systems. Based on the above work, a new constraint is added to the sparse recovery method, and the corresponding algorithm is deduced. The simulation results show that in the case of one snapshot, the method proposed in [8] cannot accurately reconstruct the sparse signal, whereas the proposed method can still recover the sparse signal robustly.

This paper is organized as follows. The sparse signal model for bistatic MIMO radar with array errors is derived in Section 2. In Section 3, a robust CS algorithm is proposed to achieve target imaging in the presence of array errors. The proposed method is tested via simulations and analysis, which appear in Section 4. Finally, Section 5 concludes the paper.

2. Signal Model of Bistatic MIMO Radar with Array Errors

The configuration of a bistatic MIMO radar is shown in Figure 1. Consider the radar has M-transmit and N-receive uniform linear array. The transmitting signals are $S \in C^{M \times L}$,

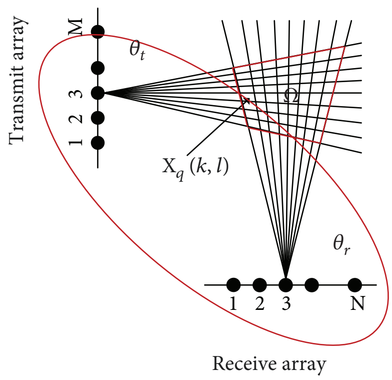

Figure 1: Bistatic MIMO radar configuration.

where L is the length of transmitting signals. Assuming that the p^{th} pixel point of the target is at the angle $(\theta_{tp}, \theta_{rp})$. The received signal can be written as

$$\mathrm{Y}_q = \mathbf{A}_r \mathbf{D}_q \mathbf{A}_t \mathbf{S} + \mathbf{E}_q \quad q = 1, 2, \dots, \mathrm{Q}, \tag{1}$$

where $\mathbf{A}_t = [\mathrm{a}_{tp}]_{M\times P}$ and $\mathrm{a}_{tp} = [1\ \mathrm{e}^{j(2\pi/\lambda)\mathrm{d}_t \sin\theta_{tp}} \mathrm{e}^{j(2\pi/\lambda)2\mathrm{d}_t \sin\theta_{tp}} \dots \mathrm{e}^{j(2\pi/\lambda)(\mathrm{M}-1)\mathrm{d}_t \sin\theta_{tp}}]$. $\mathbf{A}_r = [\mathrm{a}_{rp}]_{N\times P}$, where $\mathrm{a}_{rp} = [1\ \mathrm{e}^{j(2\pi/\lambda)\mathrm{d}_r \sin\theta_{rp}} \mathrm{e}^{j(2\pi/\lambda)2\mathrm{d}_r \sin\theta_{rp}} \dots \mathrm{e}^{j(2\pi/\lambda)(\mathrm{N}-1)\mathrm{d}_r \sin\theta_{rp}}]$. $\mathbf{A}_t$ is transmit steering matrix and $\mathbf{A}_r$ is receive steering matrix of P pixel points. λ represents the transmit signal wavelength. d_t and d_r are the ideal element space at the transmitter and receiver. $\mathbf{D}_q = \mathrm{diag}\,(d_1, \dots, d_p)$ denotes the scattering coefficient of P pixel points of the target in the qth pulse period. The noise $\mathbf{E}_q$ is assumed to be independent, and zero-mean complex Gaussian distribution with$\mathbf{E}_q \sim N^c(0, \sigma_n^2 \mathrm{I}_N)$.

As shown in Figure 1, the region of interest is divided into two dimensional discrete set of angular positions $\Omega = \{(\theta_k, \theta_l)\colon (\mathrm{k}, \mathrm{l}) \in \{1, \dots, \mathrm{G}\} \times \{1, \dots, \mathrm{G}\}\}$. The target pixel distribution is assumed to be $\mathbf{X}_q \in \mathbb{C}^{G\times G}$ and the transmit signal is orthogonal waveform. After the matched filtering, the received signal can be expressed as $\mathbf{Y}_q = \mathbf{A}_r \mathbf{X}_q \mathbf{A}_t + \mathbf{E}_q$, the vector form of it is

$$\mathbf{y_q} = \mathrm{vec}(\mathbf{Y}_q) = [\mathbf{A}_r \otimes \mathbf{A}_t]\mathrm{vec}(\mathbf{X}_q) + \mathbf{e_q} = \mathbf{A}\mathbf{x_q} + \mathbf{e_q}, \tag{2}$$

where $\mathbf{A} = \mathbf{A}_r \otimes \mathbf{A}_t$, $\mathbf{x_q} = \mathrm{vec}(\mathbf{X}_q)$, and $\mathbf{e_q} = \mathrm{vec}(\mathbf{E}_q)$. When the gain and phase errors exist for both the transmit and receive array elements, the transmit and receive steering matrix can be written as

$$\begin{aligned}\tilde{\mathbf{A}}_\mathbf{t} &= \mathbf{\Gamma_t}'\mathbf{A_t} = (\mathbf{I} + \mathbf{\Gamma_t})\mathbf{A_t} = \mathbf{A_t} + \mathbf{\Gamma_t}\mathbf{A_t} = \mathbf{A_t} + \mathbf{E_t},\\ \tilde{\mathbf{A}}_\mathbf{r} &= \mathbf{\Gamma_r}'\mathbf{A_r} = (\mathbf{I} + \mathbf{\Gamma_r})\mathbf{A_r} = \mathbf{A_r} + \mathbf{\Gamma_r}\mathbf{A_r} = \mathbf{A_r} + \mathbf{E_r},\end{aligned} \tag{3}$$

where $\mathbf{\Gamma_t} = \mathrm{diag}\,[\rho_{t1}, \dots, \rho_{tM}]$ and $\mathbf{\Gamma}_r = \mathrm{diag}\,[\rho_{r1}, \dots, \rho_{rN}]$ are the diagonal matrices with array gain and phase errors at diagonal elements. $\rho_{\mathrm{ti}} = a_{\mathrm{ti}} e^{j\varphi_{\mathrm{ti}}}$, where a_{ti} is gain error and φ_{ti} is phase error in the transmit array elements. $\rho_{\mathrm{ri}} = a_{\mathrm{ri}} e^{j\varphi_{\mathrm{ri}}}$, where a_{ri} is gain error and φ_{ri} is phase error in the receive array elements. The receiving data with the gain and phase errors of the array can be written as $\tilde{\mathbf{Y}}_q = \tilde{\mathbf{A}}_\mathbf{r} \mathbf{X}_q \tilde{\mathbf{A}}_\mathbf{t} + \mathbf{E}_q$. The vector form of it is

$$\begin{aligned}\tilde{\mathbf{y}}_\mathbf{q} &= \mathrm{vec}(\tilde{\mathbf{Y}}_q) = \left[\tilde{\mathbf{A}}_\mathbf{r} \otimes \tilde{\mathbf{A}}_\mathbf{t}\right]\mathrm{vec}(\mathbf{X}_q) + \mathbf{e_q}\\ &= [(\mathbf{A_t} + \mathbf{E_t}) \otimes (\mathbf{A_r} + \mathbf{E_r})]\mathbf{x_q} + \mathbf{e_q}\\ &= [\mathbf{A_t} \otimes \mathbf{A_r} + \mathbf{A_t} \otimes \mathbf{E_r} + \mathbf{E_t} \otimes \mathbf{A_r} + \mathbf{E_t} \otimes \mathbf{E_r}]\mathbf{x_q} + \mathbf{e_q}\\ &= (\mathbf{A} + \mathbf{E})\mathbf{x_q} + \mathbf{e_q},\end{aligned} \tag{4}$$

where

$$\mathbf{E} = \mathbf{A_t} \otimes \mathbf{E_r} + \mathbf{E_t} \otimes \mathbf{A_r} + \mathbf{E_t} \otimes \mathbf{E_r}. \tag{5}$$

It can be observed from (4) and (5) that the array error can be modeled as an additive error matrix for ideal observation matrix A. The next task is to construct the sparse recovery problem under this nonideal model.

3. Robust CS-Based Sparse Imaging Algorithm

Considering more general situation, the $\mathbf{E}$ matrix in (4) can be relaxed as a random perturbation matrix which added on the ideal observation matrix $\mathbf{A}$. Inspired by the robust beamforming method [12], the norm of the observation matrix is constrained to reduce the effect of matrix $\mathbf{E}$. A quadratic optimization problem with sparse constraint can be constructed as

$$\min_{\mathbf{B},\mathbf{x}} \left\|\tilde{\mathbf{y}}_q - \mathbf{B}\mathbf{x}\right\|_2^2 + \|\mathbf{x}\|_1 s.t \|\mathbf{B}\|_2^2 = M\|\mathbf{B} - \mathbf{A}\|_2^2 \le \varepsilon. \tag{6}$$

In this optimization problem, matrix $\mathbf{B}$ is an unknown matrix of the same size as the observation matrix $\mathbf{A}$. We use it to approximate the actual observation matrix. Since the actual observation matrix is derived from the sum of the ideal observation matrix $\mathbf{A}$ and an unknown perturbation matrix $\mathbf{E}$, we obtain more accurate values of the actual observation matrix by the above optimization methods.

The iterative method is derived to solve the optimization problem. In the k^{th} iteration, the algorithm performs two steps. In the first step, we solve the familiar convex optimization problem

$$\hat{\mathrm{x}}^{(k)} = \arg\min_{\mathrm{x}} \left\|\tilde{\mathbf{y}}_q - \mathbf{B}^{(k)}\mathbf{x}\right\|_2^2 + \|\mathbf{x}\|_1, \tag{7}$$

holding $\mathbf{B}$ matrix fixed. This is a convex optimization problem that is known to yield unique sparse solutions. The next step is to hold the coefficients x fixed and find a better observation matrix solution by using the Lagrange multiplier method. The updating formula of the observation matrix is

$$\hat{\mathbf{B}}^{(k+1)} = \left(\mathbf{y}\left(\mathbf{x}^{(k)}\right)^H + \gamma\mathbf{A}\right)\left[\mathbf{x}^{(k)}\left(\mathbf{x}^{(k)}\right)^H + (\gamma + \mu)\mathbf{I}\right]^{-1}. \tag{8}$$

The above two steps are executed iteratively until an ideal solution is obtained.

Input: $\mathbf{y}$, $\mathbf{A}$, λ, μ
Output: $\hat{\mathbf{x}}$, $\hat{\mathbf{B}}$
Step 1: Initialization: $x^0 = 0_{n\times 1}$, $\mathbf{B}^0 = \mathbf{A}$
Step 2: Fix $\mathbf{B}$ and solve the optimization problem
$\hat{x}^{(k)} = \arg \min_{x} \|\tilde{\mathbf{y}}_q - \mathbf{B}^{(k)}\mathbf{x}\|_2^2 + \|\mathbf{x}\|_1$.
Step 3: Fix $\mathbf{x}$ and calculate the matrix $\mathbf{B}$
$\hat{\mathbf{B}}^{(k+1)} = (\mathbf{y}(\mathbf{x}^{(k)})^H + \gamma\mathbf{A})[\mathbf{x}^{(k)}(\mathbf{x}^{(k)})^H + (\gamma+\mu)\mathbf{I}]^{-1}$.
Step 4: Judge the condition of convergence
$\|\mathbf{x}^{(k+1)} - \mathbf{x}^{(k)}\|_2^2 \le \varepsilon$.
If the condition is satisfied, the iteration is stopped, and Step 2 is returned if it is not satisfied.

Algorithm 1: Algorithm Flow.

In the end, we introduce the derivation of the updating formula for observation matrix. We construct the Lagrange function according to the optimization problem

$$f(\mathbf{B}, \gamma, \mu) = \|y - \mathbf{B}x\|_2^2 + \|\mathbf{x}\|_1 + \gamma\left(\|\mathbf{B} - \mathbf{A}\|_2^2 - \varepsilon\right) + \mu\left(\|\mathbf{B}\|_2^2 - M\right). \tag{9}$$

By getting the partial derivative of the Lagrange function to $\mathbf{B}$ and making it equal to zero, the optimal estimation of the actual observation matrix can be obtained.

$$\frac{\partial f}{\partial \mathbf{B}} = \frac{\partial\|\mathbf{y} - \mathbf{Bx}\|_2^2}{\partial \mathbf{B}} + \gamma\frac{\partial\|\mathbf{B} - \mathbf{A}\|_2^2}{\partial \mathbf{B}} + \mu\frac{\partial\|\mathbf{B}\|_2^2}{\partial \mathbf{B}}. \tag{10}$$

The first item is

$$\begin{aligned}\frac{\partial\|\mathbf{y} - \mathbf{Bx}\|_2^2}{\partial \mathbf{B}} &= \frac{\partial Tr\left[(\mathbf{y} - \mathbf{Bx})(\mathbf{y} - \mathbf{Bx})^H\right]}{\partial \mathbf{B}} \\ &= \frac{\partial Tr\left(\mathbf{yy}^H\right)}{\partial \mathbf{B}} - \frac{\partial Tr\left(\mathbf{yx}^H\mathbf{B}^H\right)}{\partial \mathbf{B}} \\ &\quad - \frac{\partial Tr\left(\mathbf{Bxy}^H\right)}{\partial \mathbf{B}} + \frac{\partial Tr\left(\mathbf{Bxx}^H\mathbf{B}^H\right)}{\partial \mathbf{B}} \\ &= \mathbf{0} - \mathbf{yx}^H - \left(\mathbf{xy}^H\right)^H + \mathbf{B}\left(\mathbf{xx}^H\right)^H + \mathbf{Bxx}^H \\ &= 2\mathbf{Bxx}^H - 2\mathbf{yx}^H.\end{aligned} \tag{11}$$

The second item is

$$\begin{aligned}\frac{\partial\|\mathbf{B} - \mathbf{A}\|_2^2}{\partial \mathbf{B}} &= \frac{\partial Tr\left[(\mathbf{B} - \mathbf{A})(\mathbf{B} - \mathbf{A})^H\right]}{\partial \mathbf{B}} \\ &= \frac{\partial Tr\left(\mathbf{BB}^H\right)}{\partial \mathbf{B}} - \frac{\partial Tr\left(\mathbf{BA}^H\right)}{\partial \mathbf{B}} \\ &\quad - \frac{\partial Tr\left(\mathbf{AB}^H\right)}{\partial \mathbf{B}} + \frac{\partial Tr\left(\mathbf{AA}^H\right)}{\partial \mathbf{B}} \\ &= 2\mathbf{B}\text{-}\mathbf{A}\text{-}\mathbf{A} + 0 = 2\mathbf{B}\text{-}2\mathbf{A}.\end{aligned} \tag{12}$$

The third item is

$$\frac{\partial\|\mathbf{B}\|_2^2}{\partial \mathbf{B}} = 2\mathbf{B}. \tag{13}$$

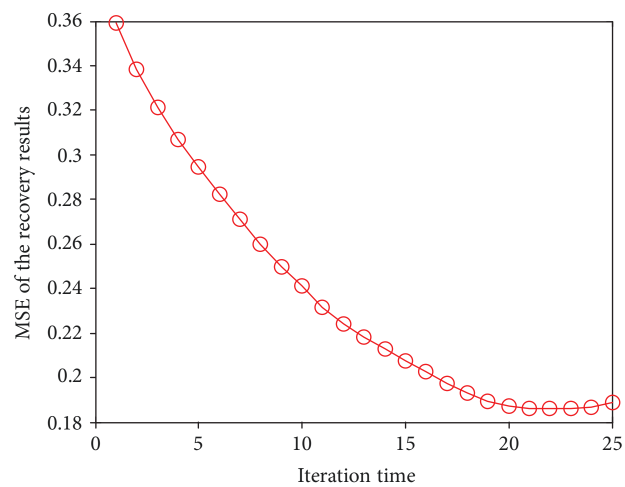

Figure 2: MSE curve with iteration time ($M = N = 15$, $Q = 1$, SNR = 10 dB, $\sigma_t = \sigma_r = 0.2$).

Table 1: The running time of each method.

Methods	Method proposed in [8]	Proposed method	Direct CS
Runtime	0.902 s	11.205 s	0.751 s

Then, we get the estimation of the actual observation matrix.

$$\begin{aligned}\frac{\partial f}{\partial \mathbf{B}} &= 2\mathbf{Bxx}^H\text{-}2\mathbf{yx}^H + 2\gamma(\mathbf{B}\text{-}\mathbf{A}) + 2\mu\mathbf{B} = 0 \\ &\Rightarrow \hat{\mathbf{B}} = \left(\mathbf{yx}^H + \gamma\mathbf{A}\right)\left[\mathbf{xx}^H + (\gamma+\mu)\mathbf{I}\right]^{-1}.\end{aligned} \tag{14}$$

The algorithm is summarized as Algorithm 1.

For the error measurement parameter ε, we take the value according to the empirical data. Usually we set ε as one tenth of the error value of the first iteration. That is to say, our algorithm stops when the estimation error of sparse signal to one tenth of the initial estimation error. This rule leads to relative good results in practice. More appropriate selection methods remain to be further studied.

Furthermore, the method we propose is a more generally applied method. As long as the signal model can be expressed

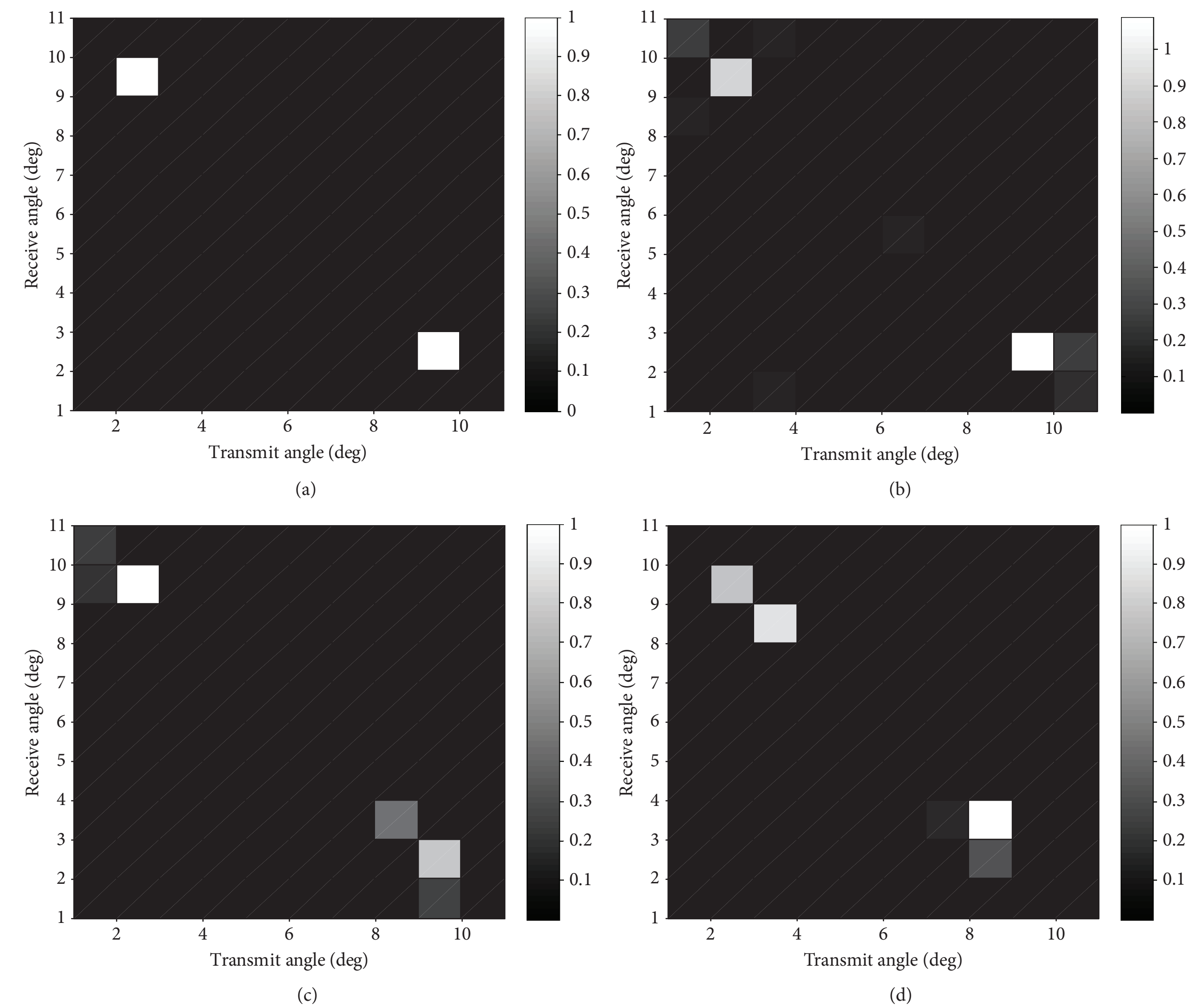

Figure 3: The performance of the proposed method compared with existing sparse methods ($M = N = 15$, $[\theta_{t1}, \theta_{r1}] = [2^\circ, 9^\circ]$, $[\theta_{t2}, \theta_{r2}] = [9^\circ, 2^\circ]$, $Q = 1$, SNR = 10 dB, $\sigma_t = \sigma_r = 0.3$, $\gamma = 0.01$). (a) Original image. (b) Proposed method ($Q = 1$, MSE = 0.26). (c) Direct CS method ($Q = 1$, MSE = 0.45). (d) Method proposed in [8] ($Q = 1$, MSE = 1.69).

as a form of random interference added to the observation matrix, the proposed method can be used for sparse reconstruction. So algorithm is still effective in the case of many nonideal situations, such as array location uncertainties, and CS grid error.

4. Simulation Results

In this section, we simulate the method proposed in this article and compare it with the method proposed in [8]. It is assumed that the transmit array element and the receive array element are uniform linear arrays with half-wavelength space between adjacent elements, and the number of transmit and receive array elements is 15. Both of the transmit angular region and receive angular region range from 1° to 10°. Assume that there are two pixels of a target at angle $[\theta_{t1}, \theta_{r1}] = [2^\circ, 9^\circ]$ and $[\theta_{t2}, \theta_{r2}] = [9^\circ, 2^\circ]$. We use only one snapshot for the sparse recovery.

The form of the transmit and receive array gain and phase error is

$$\begin{aligned} \Gamma_t &= \operatorname{diag}\left\{\exp\left[N\left(0, \sigma_t^2\right)\right] \odot \exp\left[jN\left(0, \sigma_t^2\right)\right]\right\}, \\ \Gamma_r &= \operatorname{diag}\left\{\exp\left[N\left(0, \sigma_r^2\right)\right] \odot \exp\left[jN\left(0, \sigma_r^2\right)\right]\right\}, \end{aligned} \tag{15}$$

where σ_t and σ_r are the parameters governing the array errors. $N(0, \sigma_r^2)$ denotes the Gaussian distribution. The single snapshot data is used in the simulations.

Figure 2 shows the MSE of the recovery results varying with iteration time. In the statistical sense, the algorithm converges at about 20 iteration times. The convergence rate of the algorithm is related to the size of the observation matrix and the selection of Lagrange multipliers.

Figure 3 shows the results of the image recovery using the proposed method compared with existing sparse methods. It

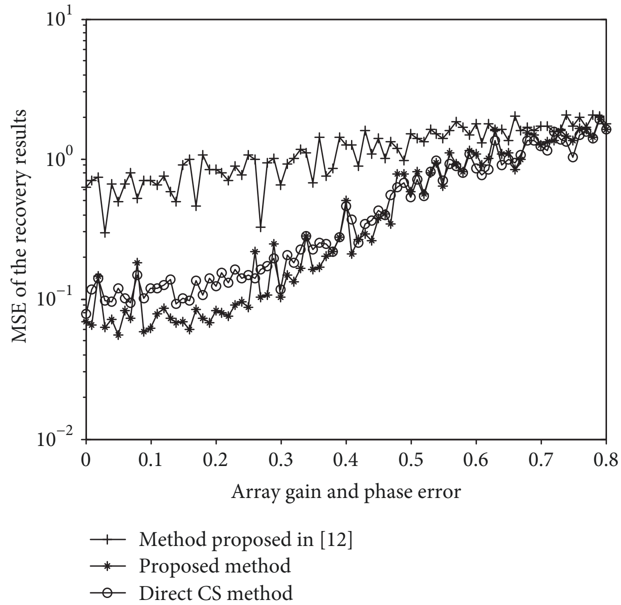

Figure 4: Comparison of the performance of sparse recovery methods.

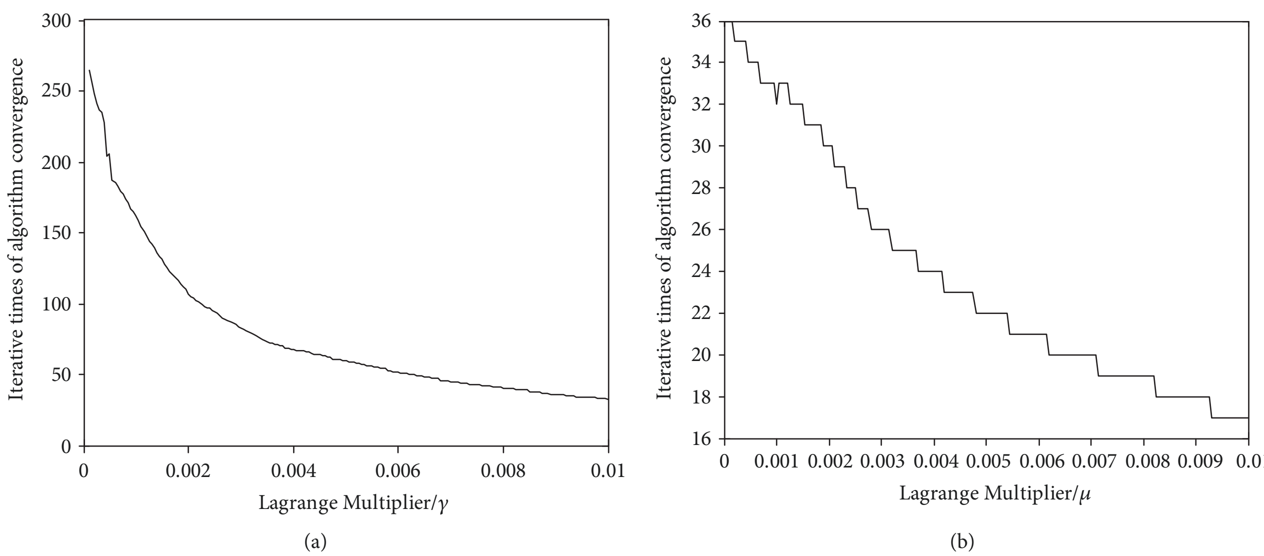

Figure 5: The influence of parameters on the convergence of the algorithm. (a) Convergent curve ($\mu = 0.001$). (b) Convergent curve ($\gamma = 0.01$).

can be observed that the image recovery of the direct CS method and the algorithm proposed in [8] have relatively higher sidelobes. It is obvious that the performance of the proposed method is prior to both of them.

The running time of the examples in Figure 3 by MATLAB in the same computer is listed in Table 1. It can be observed that the computational complexity of the proposed method increases while it improves the performance of the sparse recovery.

Figure 4 plots the mean square error of recovery results of the proposed method, the method in [8], and the direct CS method. The governing parameters of the array errors are equal for all the elements. The array error parameter changes from 0 to 0.6 with the interval 0.01. For each simulation, 500 Monte Carlo trails are run. It is shown that the performance of the method in [8] is very poor, even worse than the direct CS method, in the case of one snapshot. The proposed method has the lowest MSE among three methods. The results confirm that the proposed method is robust for array errors and suitable to one snapshot case. It can be observed from Figure 4 that the performance of the proposed method is degraded when the array gain and phase errors are greater than 0.4. The result implies that the proposed method is applicable in the case of relatively small array gain and phase errors.

Figure 5 (a) shows the effect of γ on the convergence of the algorithm. The parameter μ is set as 0.001 and γ increases from 0.0001 to 0.01 with the interval 0.00005. For each γ, 100 simulations are performed to get the average number of iterations required for convergence of the algorithm. The same simulations are done to evaluate the effect of μ on the convergence of the algorithm in Figure 5 (b). It is shown that the iteration number will be small with the increase of γ and μ. However, too large γ and μ will result to the divergence of the algorithm.

5. Conclusions

A robust transmit-receive angle imaging method for bistatic MIMO radar based on CS had been proposed in this paper. The method can be used to enhance the performance of CS in the case of both gain and phase errors of the array. In addition, only one snapshot is required in the proposed method. Simulation and analysis demonstrated the effectiveness of the proposed method.

Data Availability

The simulation data used to support the findings of this study are included within the article.

Conflicts of Interest

The authors declare that they have no competing interests.

Acknowledgments

This study has been supported by the National Natural Science Foundation of China under Contract no. 61431016.

References

[1] I. Bekkerman and J. Tabrikian, "Target detection and localization using MIMO radars and sonars," *IEEE Transactions on Signal Processing*, vol. 54, no. 10, pp. 3873–3883, 2006.

[2] J. L. Chen, "A method for fast multi-target localization in bistatic MIMO radar system," *Journal of Electronics & Information Technology*, vol. 31, no. 7, pp. 1664–1668, 2009.

[3] J. Chen, H. Gu, and W. Su, "A new method for joint DOD and DOA estimation in bistatic MIMO radar," *Signal Processing*, vol. 90, no. 2, pp. 714–718, 2010.

[4] J. F. Li, W. Y. Chen, and X. F. Zhang, "Angle estimation for bistatic MIMO radar with unknown mutual coupling based on improved propagator method," *Applied Mechanics and Materials*, vol. 513-517, pp. 3029–3033, 2014.

[5] J. Li, Y. Guo, G. Liao, Q. Guo, and J. Xi, "Dimension reduced sparse recovery method for clutter suppression in bistatic MIMO radar," in *2015 IEEE Radar Conference (RadarCon)*, Washington DC, USA, May 2015.

[6] G. Zheng, D. Zhang, Y. Zhang, J. Tang, C. Feng, and X. Hu, "Fast OMP algorithm for 3D parameters super-resolution estimation in bistatic MIMO radar," *Electronics Letters*, vol. 52, no. 13, pp. 1164–1166, 2016.

[7] N. Tong, Y. Zhang, G. Hu, X. He, and X. Hu, "Multiple-input–multiple-output radar super-resolution three-dimensional imaging based on a dimension-reduction compressive sensing," *IET Radar, Sonar & Navigation*, vol. 10, no. 4, pp. 757–764, 2016.

[8] J. Li, S. Zhu, X. Chen, L. Lv, G. Liao, and M. Yi, "Sparse recovery for bistatic MIMO radar imaging in the presence of array gain uncertainties," *International Journal of Antennas and Propagation*, vol. 2014, no. 1, Article ID 807960, 6 pages, 2014.

[9] Y. Chi, L. L. Scharf, A. Pezeshki, and A. R. Calderbank, "Sensitivity to basis mismatch in compressed sensing," *IEEE Transactions on Signal Processing*, vol. 59, no. 5, pp. 2182–2195, 2011.

[10] G. Tang, B. N. Bhaskar, P. Shah, and B. Recht, "Compressed sensing off the grid," *IEEE Transactions on Information Theory*, vol. 59, no. 11, pp. 7465–7490, 2013.

[11] H. Zhu, G. Leus, and G. B. Giannakis, "Sparsity-cognizant total least-squares for perturbed compressive sampling," *IEEE Transactions on Signal Processing*, vol. 59, no. 5, pp. 2002–2016, 2011.

[12] J. Li, P. Stoica, and Z. Wang, "Doubly constrained robust Capon beamformer," *IEEE Transactions on Signal Processing*, vol. 52, no. 9, pp. 2407–2423, 2004.